Analyses of the collective properties of hadronic matter in Au-Au collisions at 54.4 GeV

M. Waqas[1,*] G. X. Peng[1,2,†] M. Ajaz[3,‡] A. Haj Ismail[4,5] and E. A. Dawi[4,5]

[1]*School of Nuclear Science and Technology, University of Chinese Academy of Sciences, Beijing 100049, China*
[2]*Theoretical Physics Center for Science Facilities, Institute of High Energy Physics, Beijing 100049, China*
[3]*Department of Physics, Abdul Wali Khan University Mardan, Mardan 23200, Pakistan*
[4]*Department of Mathematics and Science, Ajman University, Ajman 346, United Arab Emirates*
[5]*Nonlinear Dynamics Research Center (NDRC), Ajman University, Ajman 346, United Arab Emirates*

We investigated the strange hadrons transverse momentum (p_T) spectra in Au-Au collision at $\sqrt{s_{NN}} =$ 54.4 GeV in the framework of modified Hagedorn function with embedded flow. It is found that the model can describe the particle spectra well. We extracted the kinetic freeze-out temperature T_0, transverse flow velocity β_T, kinetic freeze-out volume V, mean transverse momentum $\langle p_T \rangle$, the entropy parameter n, and the multiplicity parameter N_0. We reported that all these parameters increase towards the central collisions. The larger kinetic freeze-out temperature, transverse flow velocity, kinetic freeze-out volume, and the entropy parameter (n) in central collisions compared to peripheral collisions show the early decoupling of the particles in central collisions. In addition, all the above parameters are mass dependent. The kinetic freeze-out temperature (T_0), the entropy parameter n, and mean transverse momentum ($\langle p_T \rangle$) are larger for massive particles, while the transverse flow velocity (β_T), kinetic freeze-out volume (V), and the multiplicity parameter (N_0) show the opposite behavior. Larger T_0, n, and smaller β_T as well as V of the heavier particles indicate the early freeze-out of the heavier particles, while larger $\langle p_T \rangle$ for the heavier particles evince that the effect of radial flow is stronger in heavier particles. The separate set of parameters for each particle shows the multiple kinetic freeze-out scenario, where the mass-dependent kinetic freeze-out volume shows the volume differential freeze-out scenario. We also checked the correlation among different parameters, which include the correlation of T_0 and β_T, T_0 and V, β_T and V, $\langle p_T \rangle$ and T_0, $\langle p_T \rangle$ and β_T, $\langle p_T \rangle$, and V, n and T_0, n and β_T, and n and V, and they all are observed to have positive correlations with each other which validates our results.

DOI: 10.1103/PhysRevD.106.075009

I. INTRODUCTION

Heavy-ion collisions at the ultrarelativistic energies provide a strong evidence [1–5] for a novel phase of quantum chromodynamics (QCD) matter, which is called quark gluon plasma (QGP) [6–10]. Many approaches [11–23] have been developed to study the QGP matter in order to understand the laws of nature at subatomic level,

[*]waqas_phy313@yahoo.com
[†]Corresponding author.
gxpeng@ucas.ac.cn
[‡]Corresponding author.
ajaz@awkum.edu.pk

but due to its short lifetime its direct measurement is very difficult. However, the dynamical models can play a vital role to explore this provoking and exciting phenomenon happening in the early stages of interaction. Nonetheless, it is understandable that the indirect investigation depends on the excellence of the model to repeatedly and precisely reestablish the related dynamics and phases of the collision from hadron formation to their detection.

Temperature (T) versus baryon chemical potential (μ_B) is usually plotted to show the phase diagram of QCD. In heavy-ion collisions, the evaluation of particle yields and their resemblance to the statistical models suggest that T and μ_B differ in an inverse manner with the center of mass energy ($\sqrt{s_{NN}}$) at the chemical freeze-out [24]. T increases with $\sqrt{s_{NN}}$ while μ_B decreases [25]. Therefore, by varying $\sqrt{s_{NN}}$, the two axes of the phase diagram T and μ_B, can be changed, and get access to a large part of the phase space experimentally. For the study of the phase structure of QCD phase diagram, the Beam Energy Scan (BES)

program [26–28] has been designed. Among the different $\sqrt{s_{NN}}$, the STAR experimental group also collected high statistics data for Au-Au collisions at 54.4 GeV in 2017, which allows us to extend the accurate measurements of different observables especially from intermediate to high p_T [29].

There are many kinds of temperatures studied in literature which includes the initial temperature (T_i) [30,31], chemical freeze-out temperature (T_{ch}) [32–34], effective temperature (T) [35–38], and kinetic freeze-out temperature (T_0) [39–42]. These temperatures correspond to different stages of evolution. Since the selection of the modified Hagedorn function with embedded flow [43] in the present work due to its closeness to the ideal gas model is brought under consideration, which describes the final state properties of the particles. Therefore we are not interested in other temperatures except the kinetic freeze-out temperature.

Kinetic freeze-out of particles is a very complex phenomenon. Different literatures provide the evidence of different kinetic freeze-out scenarios. For instance Ref. [44] shows the single kinetic freeze-out scenario, Ref. [45–47] shows double kinetic freeze-out scenario, and similarly Ref. [48–50] shows the multiple kinetic freeze-out scenario. In our recent work [51], we also observed a triple kinetic freeze-out scenario, where we studied nonstrange, strange, and multistrange particles and found that the multistrange particles freeze-out early than the nonstrange and strange particles. It also increases our curiosity to study the charm particles in future, and we expect their earlier freeze-out than the multistrange particles. Though there are different opinions about the freeze-out scenarios but it is still an open question in the community. Furthermore, the dependence of the kinetic freeze-out temperature (T_0) from central to peripheral collision has different studies. Several literatures claim the decrease of T_0 with increasing centrality [52,53] which suggests the longer-lived fireball in central collisions. However, according to some literature [21,31,39,50,54,55], T_0 decreases with decreasing centrality which suggests the higher degree of excitation of the system in central collisions. This is also an open question in the community up to now. Both the trends of increasing or decreasing of T_0 with centrality are correct in their own explanations.

The transverse momentum (p_T) spectra of the particles are very significant observables in high-energy collisions, and they can be used for the scrutiny of the dynamics of the particle production. In the present work, we analyze the p_T spectra of strange particles (k_s^0, Λ, $\bar{\Lambda}$, $\bar{\Xi}^+$, and Ξ^-) by the modified Hagedorn function with embedded flow [43], and extracted the bulk properties of matter in terms of kinetic freeze-out temperature, transverse flow velocity, and kinetic freeze-out volume.

The remainder of the paper consists of method and formalism followed by the results and discussions and then conclusions.

II. THE METHOD AND FORMALISM

In high-energy collisions, it is a known fact that the high p_T part of transverse momentum spectra of the particles is well described by the QCD inspired Hagedorn function [56]

$$\frac{1}{N}\frac{d^2N}{2\pi p_T dp_T dy} = C\left(1 + \frac{m_T}{p_0}\right)^{-n}, \quad (1)$$

where N represents the number of charged particles of a particular type, p_T is the transverse momentum spectra, "C" is constant of normalization, p_0 and n are the free parameters, m_T is the transverse mass and can be expressed as $m_T = \sqrt{(m_0)^2 + (p_T)^2}$, and m_0 is the rest mass of the hadron species.

As we know that the invariant p_T and m_T distribution of the particles in high-energy collisions at RHIC and LHC [57–64] can be well described by the Tsallis distribution function [65,66]. There are many versions of Tsallis function [64,67–71] and its more simplified version at midrapidity is

$$\frac{1}{N}\frac{d^2N}{2\pi p_T dp_T dy} = C\left(1 + (q-1)\frac{m_T}{T}\right)^{-1/(q-1)}, \quad (2)$$

where T is the effective temperature, and q is the entropy based parameter which characterizes the degree of deviation of the p_T distribution from exponential Boltzmann-Gibbs dsitribution. Equation (2) is the nonextensive generalized form of the exponential Boltzmann distribution which introduces a new parameter q to the temperature.

The Tsallis distribution function at midrapidity can also be expressed [57,63,64] as

$$\frac{1}{N}\frac{d^2N}{2\pi p_T dp_T dy} = Cm_T\left(1 + (q-1)\frac{m_T}{T}\right)^{-q/(q-1)}, \quad (3)$$

which is a thermodynamically consistent Tsallis function.

Equations (1) and (2) are mathematically equivalent if $n = 1/(q-1)$ and $p_0 = nT_0$. It should be noted that here T_0 is the kinetic freeze-out temperature. T used in Eqs. (1)–(3) is the effective temperature which can be expressed as $T = T_0 + \langle\beta_T\rangle$ [72]. By inserting p_0 in Eq. (1), we have

$$\frac{1}{N}\frac{d^2N}{2\pi p_T dp_T dy} = C\left(1 + \frac{m_T}{nT_0}\right)^{-n}. \quad (4)$$

According to Ref. [67,73–75], the transverse flow is introduced in Eq. (4)

$$\frac{1}{N}\frac{d^2N}{2\pi p_T dp_T dy} = C\left(1 + \frac{\langle\gamma_T\rangle(m_T - p_T\langle\beta_T\rangle)}{nT_0}\right)^{-n}, \quad (5)$$
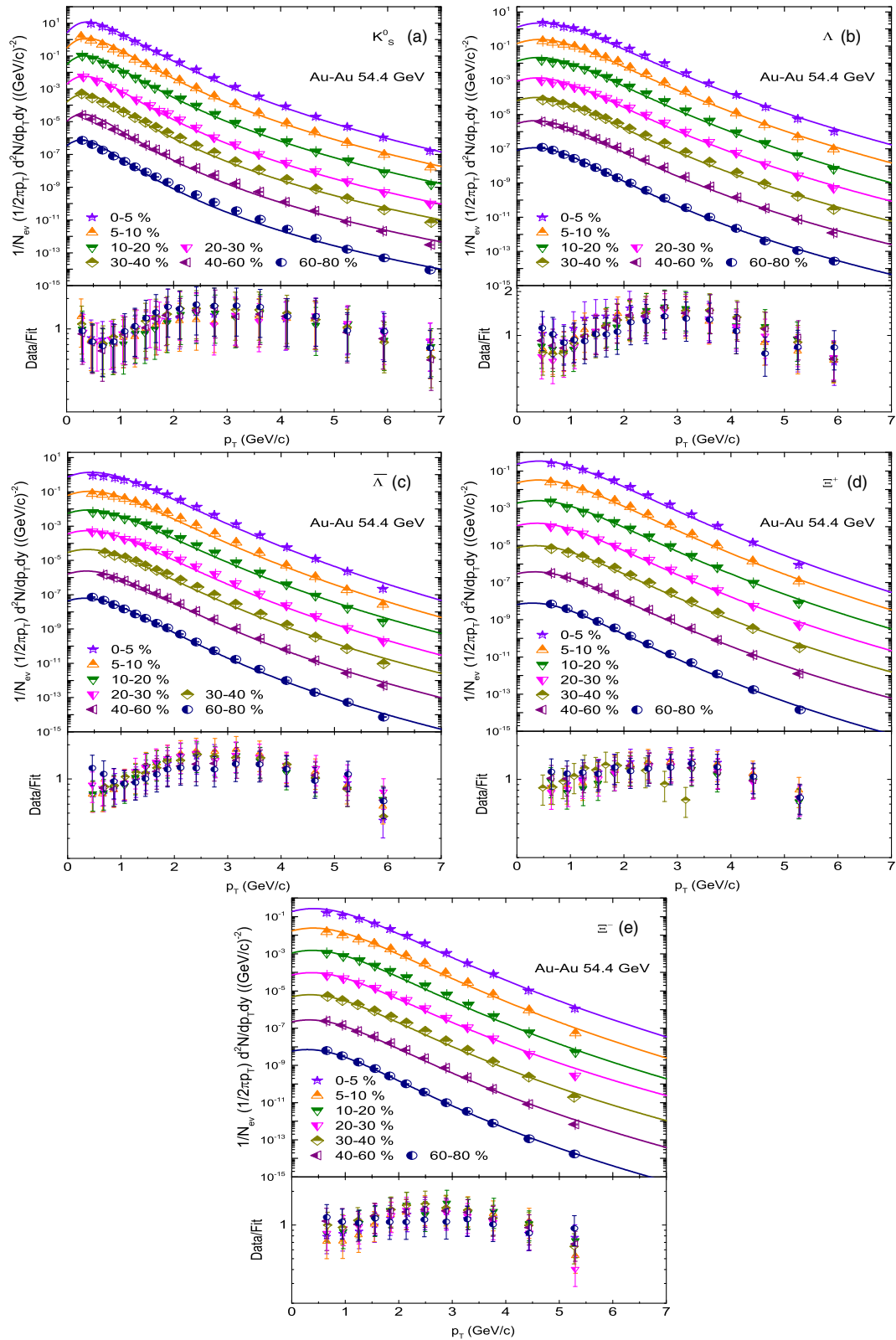
FIG. 1. Transverse momentum spectra of k_s^0, Λ, $\bar{\Lambda}$, $\bar{\Xi}^+$, and Ξ^- in Au-Au collisions at 54.4 GeV. The data points are the experimental data of STAR Collaboration [29] while curves show our fit results by Eq. (6). Each panel consists its data/fit ratios in their lower part.

where $\gamma_t = 1/\sqrt{1 - \langle\beta_T\rangle^2}$, $\langle\beta_T\rangle$ denotes the average transverse-flow velocity, T_0 represents the kinetic freeze-out temperature. In the present work, Eq. (5) is known as the Hagedron function with embedded flow [67,73–76] and it covers the low- as well as the high-p_T regions. The Hagedron function with embedded flow in Eq. (5) is modified as

$$\frac{1}{N}\frac{d^2N}{dp_T dy} = 2\pi p_T C\left(1 + \frac{\langle\gamma_T\rangle(m_T - p_T\langle\beta_T\rangle)}{nT_0}\right)^{-n}. \quad (6)$$

In the present work, we have used Eq. (6) for the individual fit of the particles.

III. RESULTS AND DISCUSSION

The STAR Collaboration [29] had reported the spectra of strange hadrons (k_s^0, Λ, $\bar{\Lambda}$, $\bar{\Xi}^+$, and Ξ^-) produced in Gold-Gold (Au-Au) collisions at $\sqrt{s_{NN}} = 54.4$ GeV in various centrality intervals for midrapidity region of $|y| < 0.5$. Figure 1 panels (a)–(e) display the p_T spectra of k_s^0, Λ, $\bar{\Lambda}$, $\bar{\Xi}^+$, and Ξ^- respectively in different centrality classes. The centrality classes include 0–5%, 5–10%, 10–20%, 20–30%, 30–40%, 40–60%, and 60–80%. One can see different symbols in each panel which represents different centrality classes, while the curves over each data set in each panel are the results of our fitting by using the modified Hagedorn function with embedded flow.

TABLE I. Values of free parameters T_0 and β_T, V and n, normalization constant (N_0), χ^2, and d.o.f. corresponding to the curves in Fig. 1.

| Collisions	Centrality	Particle	T_0	β_T	$V(\text{fm}^3)$	n	N_0	χ^2/d.o.f.
Figure 1	0–5%	K_S^0	0.050 ± 0.005	0.620 ± 0.008	5568 ± 185	15.2 ± 0.5	3 ± 0.3	3/15
Au-Au	5–10%	K_S^0	0.047 ± 0.003	0.600 ± 0.006	5400 ± 136	14.0 ± 1.6	0.30 ± 0.03	5/16
4.4 GeV	10–20%	K_S^0	0.045 ± 0.005	0.578 ± 0.008	5225 ± 172	13.3 ± 1.6	0.025 ± 0.006	6/16
	20–30%	K_S^0	0.043 ± 0.003	0.553 ± 0.008	5158 ± 155	12.6 ± 2	0.0013 ± 0.0003	4/15
	30–40%	K_S^0	0.040 ± 0.003	0.543 ± 0.007	5000 ± 148	11.8 ± 1.4	$1E-4 \pm 3E-5$	9/16
	40–60%	K_S^0	0.037 ± 0.004	0.520 ± 0.010	4733 ± 109	11.5 ± 0.5	$6E-6 \pm 4E-7$	10/16
	60–80%	K_S^0	0.034 ± 0.005	0.482 ± 0.011	4530 ± 163	11.0 ± 1.2	$1.5E-7 \pm 5E-8$	8/16
	0–5%	Λ	0.081 ± 0.005	0.370 ± 0.008	4505 ± 130	18.5 ± 2.1	0.64 ± 0.07	12/14
	5–10%	Λ	0.078 ± 0.003	0.360 ± 0.007	4300 ± 176	18.2 ± 1.7	0.07 ± 0.004	11/14
	10–20%	Λ	0.075 ± 0.003	0.340 ± 0.007	4136 ± 100	17.7 ± 1.2	0.006 ± 0.0005	11.4/14
	20–30%	Λ	0.070 ± 0.004	0.323 ± 0.010	4000 ± 101	16.3 ± 1.4	$3.8E-4 \pm 4E-5$	13.5/14
	30–40%	Λ	0.063 ± 0.005	0.310 ± 0.007	3800 ± 111	15.4 ± 1.3	$2.7E-5 \pm 5E-6$	13/14
	40–60%	Λ	0.058 ± 0.005	0.300 ± 0.011	3639 ± 121	14.8 ± 1	$1.2E-6 \pm 3E-7$	9/14
	60–80%	Λ	0.052 ± 0.004	0.280 ± 0.008	3500 ± 154	14.4 ± 1.4	$3E-8 \pm 4E-9$	5/14
	0–5%	$\bar{\Lambda}$	0.081 ± 0.005	0.370 ± 0.008	4505 ± 130	20 ± 2.3	0.38 ± 0.05	30.7/14
	5–10%	$\bar{\Lambda}$	0.078 ± 0.004	0.355 ± 0.009	4313 ± 170	18.6 ± 1.5	0.03 ± 0.003	23/14
	10–20%	$\bar{\Lambda}$	0.075 ± 0.003	0.330 ± 0.010	4136 ± 103	17.0 ± 1.2	0.0024 ± 0.0003	16/14
	20–30%	$\bar{\Lambda}$	0.070 ± 0.005	0.323 ± 0.010	4000 ± 109	16.5 ± 1.5	$1.5E-4 \pm 3E-5$	123/14
	30–40%	$\bar{\Lambda}$	0.063 ± 0.005	0.310 ± 0.007	3800 ± 111	15.4 ± 1.3	$1.2E-5 \pm 4E-6$	25/14
	40–60%	$\bar{\Lambda}$	0.058 ± 0.005	0.300 ± 0.011	3639 ± 121	15.2 ± 1.1	$6.5E-7 \pm 4E-8$	10/14
	60–80%	$\bar{\Lambda}$	0.052 ± 0.004	0.280 ± 0.008	3500 ± 154	15 ± 1.2	$1.6E-8 \pm 5E-9$	8/14
	0–5%	$\bar{\Xi}^+$	0.104 ± 0.004	0.300 ± 0.007	3700 ± 110	22 ± 2.8	0.13 ± 0.06	10/9
	5–10%	$\bar{\Xi}^+$	0.098 ± 0.005	0.290 ± 0.009	3580 ± 125	20.3 ± 2.1	0.0125 ± 0.004	6/9
	10–20%	$\bar{\Xi}^+$	0.094 ± 0.004	0.279 ± 0.008	3400 ± 120	19 ± 2.1	0.001 ± 0.0003	7.5/9
	20–30%	$\bar{\Xi}^+$	0.090 ± 0.003	0.268 ± 0.007	3200 ± 140	18 ± 1.5	$6.2E-5 \pm 4E-6$	7/9
	30–40%	$\bar{\Xi}^+$	0.087 ± 0.005	0.250 ± 0.010	3110 ± 110	17 ± 1.1	$3.8E-6 \pm 3E-7$	7/9
	40–60%	$\bar{\Xi}^+$	0.084 ± 0.004	0.240 ± 0.011	3000 ± 100	16.5 ± 1.3	$1.5E-7 \pm 4E-8$	5/9
	60–80%	$\bar{\Xi}^+$	0.079 ± 0.005	0.214 ± 0.008	2800 ± 120	16.4 ± 1.3	$3E-9 \pm 3E-10$	6/9
	0–5%	Ξ^-	0.104 ± 0.005	0.300 ± 0.007	3700 ± 115	21.1 ± 2.1	0.11 ± 0.04	5.5/9
	5–10%	Ξ^-	0.098 ± 0.003	0.290 ± 0.008	3580 ± 120	20.3 ± 2.1	0.0093 ± 0.0006	17/9
	10–20%	Ξ^-	0.094 ± 0.005	0.279 ± 0.008	3400 ± 120	19 ± 2.1	$6E-4 \pm 4E-5$	7.5/9
	20–30%	Ξ^-	0.090 ± 0.005	0.268 ± 0.010	3200 ± 118	17 ± 1.2	$4E-5 \pm 5E-6$	28/9
	30–40%	Ξ^-	0.087 ± 0.004	0.250 ± 0.009	3110 ± 117	16.9 ± 1.2	$2.5E-6 \pm 4E-7$	9/9
	40–60%	Ξ^-	0.084 ± 0.004	0.240 ± 0.011	3000 ± 100	16.7 ± 1.3	$1.1E-7 \pm 6E-8$	6.5/9
	60–80%	Ξ^-	0.079 ± 0.005	0.214 ± 0.008	2800 ± 120	16.5 ± 1.1	$2.7E-9 \pm 4E-10$	1/9
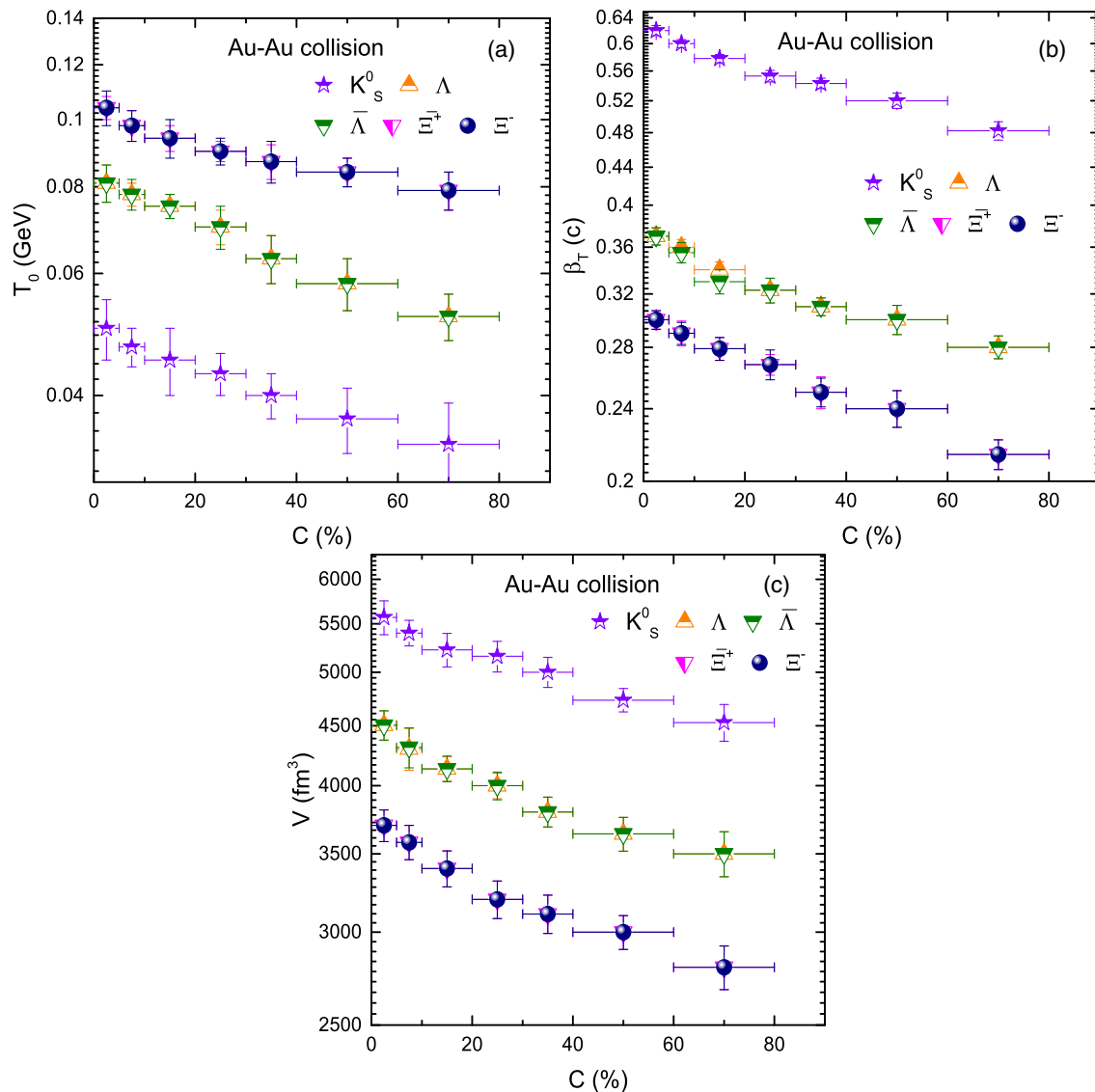
FIG. 2.   Dependence of (a) T_0, (b) β_T, and (c) V on centrality as well as m_0.

The approximately well fit of the STAR data in mid-rapidity in Au-Au collisions by Eq. (6) can be seen. The lower panels show the data/fit ratios of the corresponding upper panel to monitor the quality of the fits. To confirm the firmness of the obtained parameter values, the fit procedure is repeated three times, changing the initial values of parameters. As a result, the stability of the obtained parameters (they have stayed practically the same) has been fully validated. The extracted values of the free parameters, normalization constant (N_0), χ^2, and degrees of freedom (d.o.f.) are listed in Table I.

In order to explore more intuitively the dependence of the parameters on centrality, mass or their mutual correlation, we introduced Figs. 2–7, where the parameters are cited from Table I. Figure 2 shows the results of kinetic freeze-out temperature (T_0), transverse flow velocity (β_T), and kinetic freeze-out volume (V). In Fig. 2(a), T_0 as a

function of centrality class and m_0 are displayed. Different symbols are used to represent different particle species, and the trend of the symbols from left to right show the trend of the parameters from central to peripheral collisions. It is reported that T_0 is larger for central collisions (0–5%) and decreases with decrease of centrality.

The central collisions correspond to the creation of higher-concentration energies due to the large number of participants involved in the reaction and hence it results in a larger T_0. However, as the system moves toward the periphery, the created concentration energies becomes less and less and thus, it results in smaller T_0. This result is consistent with our previous work [31,50,51,54,76]. Reference [31,77] shows larger T_0 where T_0 is extracted by an alternative method in different collision systems for the nonstrange particles. In Ref. [51] we analyzed non-strange, strange, and multistrange particles, and in Ref. [50]
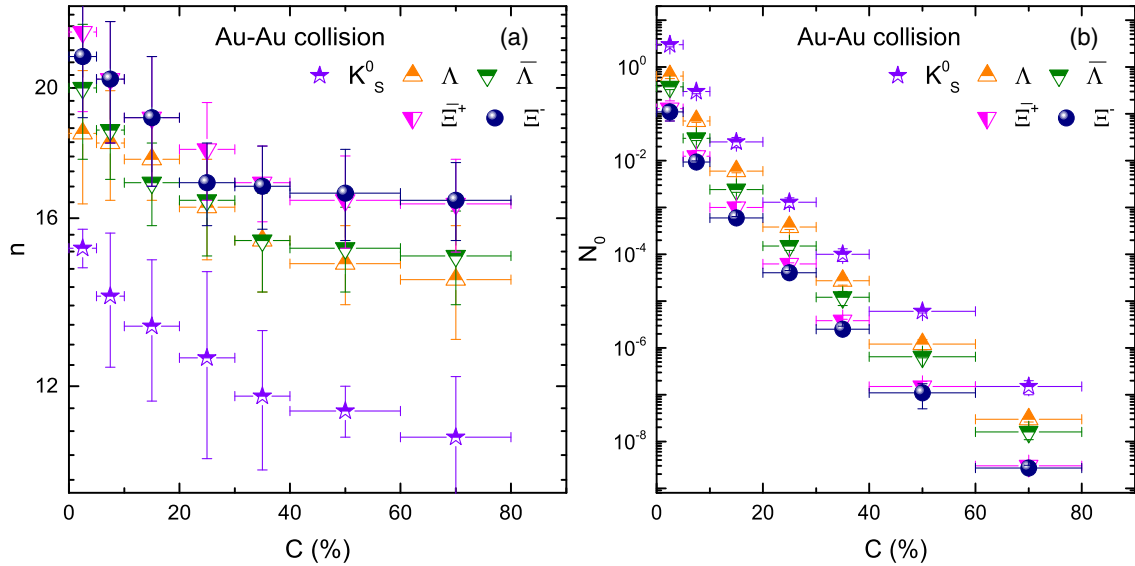
FIG. 3. Dependence of (b) n and (b) N_0 on centrality as well as m_0.

light nuclei are studied by different models respectively in narrow p_T range, and the result for T_0 is larger in central collisions. The increasing or decreasing trend of T_0 with centrality is a complex scenario. It sometimes depends on the model, sometimes it depend on other factors like the flow profile in some models and p_T range. Besides, T_0 reveals the mass differential kinetic freeze-out scenario, as it is larger for the massive particles such that $k_s^0 < \Lambda < \Xi$ (where Λ stands for Λ, $\bar{\Lambda}$, and Ξ stands for $\bar{\Xi}^+$ and Ξ^-). We also believe that this larger T_0 for Ξ than Λ and k_s^0, similarly larger T_0 for Λ than k_s^0 maybe due to different quark

contents or maybe quark flavors such as $d\bar{s}$ for k_s^0, uds for Λ and ssd for Ξ. However to confirm it, we need more particles with different quark combinations and different quarks flavors, which we will do in future. It is noteworthy that T_0 for Λ, and $\bar{\Lambda}$, and for Ξ and $\bar{\Xi}^+$ is equal which means that they have equal interaction with medium produced in the collisions respectively.

Figure 2(b) shows the transverse flow velocity β_T dependence on centrality class and m_0. We reported that the collective behavior at the kinetic freeze-out stage changes with centrality. The central collisions experience very harsh squeeze which deposits more energy per nucleon in the system that results in a rapid expansion of the fireball, while the squeeze becomes less violent as the system goes towards periphery and the amount of energy deposition in the system becomes less, and the expansion of the fireball becomes steady, which results in lower values of β_T in peripheral collisions. We believe that the flow is produced in the inner core of the interacting system, therefore even for the peripheral collisions the flow velocity is nonzero. One can see that there exists a clear partition of β_T among different centralities, such that β_T is larger in most central collisions, while it is the lowest in most peripheral collisions, and it comes in between in intermediate centralities which renders that most central collision result in high pressure gradients and therefore larger velocities of produced particles flying out from this zone at expansion stage. We also reported that β_T shows mass dependency. The lighter the mass of the particle, the higher will be the transverse-flow velocity and vice versa. The reason behind this is that the heavier particles are left behind in this system due to its large inertia and comes out later; however, the light particles due to their small inertia come out of the system early.
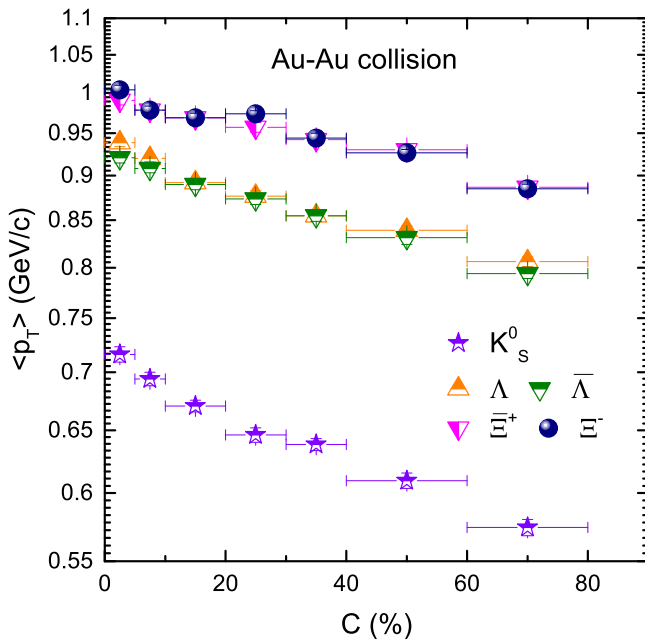

FIG. 4. Dependence of $\langle p_T \rangle$ on centrality as well as m_0.

Figure 2(c) displays the kinetic freeze-out volume (V) as a function of centrality and m_0. Like T_0 and β_T, it also grows towards the central collisions. Large number of participants involved in interaction in central collisions which correspond to large number of binary collisions by the rescattering of partons that bring the system to equilibrium state quickly. While the number of participants reduces in peripheral collisions and the system reaches equilibrium state in a steady manner. In addition to these observations, V also depends on the mass of the particles. The lighter the mass of the particle, the higher the value of V is, which renders the early freeze-out of massive particles. This indicates that there is a separate freeze-out surface for each particle and renders a volume differential freeze-out scenario. In the present work, Ξ has the lowest V which renders its early freeze-out.

Figure 3 shows the parameter n and N_0 dependence on centrality and mass of the particle in Au-Au collisions for k_s^0, Λ, $\bar{\Lambda}$, $\bar{\Xi}^+$ and Ξ^- strange particles. Figure 3(a) shows the result of the dependence of the parameter n on centrality and m_0, where as Fig. 3(b) shows the result for the parameter N_0. In Fig. 3(a), the parameter n is an entropy based parameter and is given as $n = 1/(q-1)$. n is referred for the degree of equilibrium or nonequilibrium. As a reciprocal of q, large n corresponds to equilibrium. The larger the value of n, the closer the system will be to equilibrium state. Usually, the parameter $q = 1$ refers to equilibrium state, and $q > 1$ corresponds to the nonequilibrium state. It can be seen that n increases with the increase of centrality which means that the central collisions are more close to equilibrium state. Furthermore, n is also observed to be dependent on the particle species, For
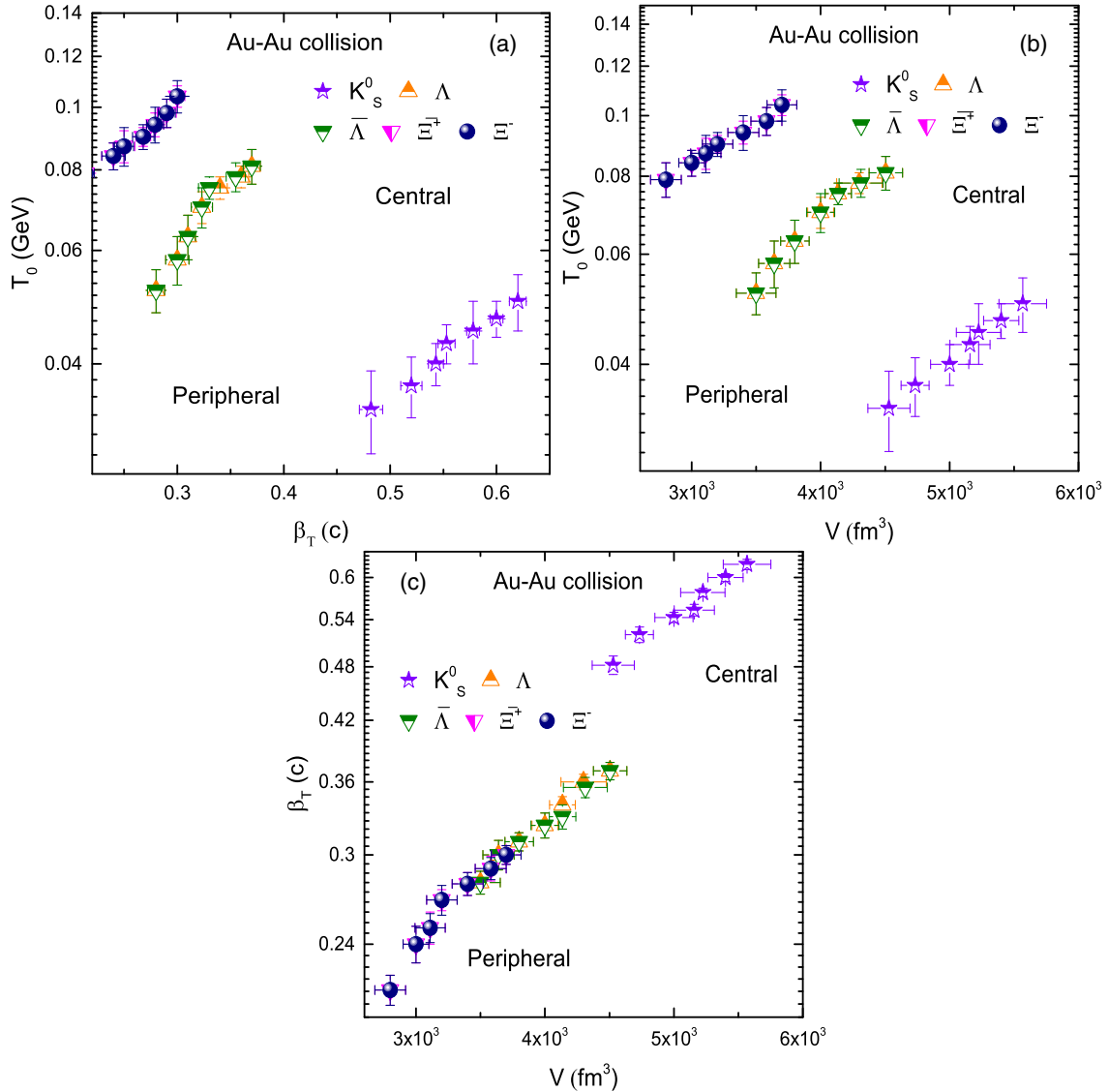

FIG. 5.   Correlation of T_0 versus β_T, T_0 versus V, and β_T versus V.

instance, smaller values of n can be seen for lighter particle (K_s^0), which indicates K_s^0 interaction with the medium produced in collisions is less and comes to equilibrium very steadily. However, $\bar{\Xi}^+$ and Ξ^- have larger values of n which naturally means to interact more with the produced medium during the collision and therefore they have a quick approach to equilibrium state. It should be noted that the physical restrictions on the parameter values have been imposed by us during the fitting procedure. For instance T_0 for K_s^0 was allowed to vary between 0.034 to 0.050 GeV, and n was restricted to the range from 11 to 15.2. Similarly T_0 for Λ and Ξ are restricted to change between 0.052 GeV to 0.081 GeV, and 0.089 GeV to 0.104 GeV respectively while n changes from 14.4 to 20, and 16.4 to 22.

Figure 3(b) displays the dependence of the multiplicity parameter N_0 on centrality and m_0. N_0 is basically the normalization constant which is used to compare the fit function with the experimental spectra, but it has a physical significance. It shows the multiplicity. Here it should be noted that we discussed the normalization constant C in Eq. (1), but C is different from N_0, because C is used to lead the integral of Eq. (1) to be normalized to unity. The sole purpose of the interpretation of both C and N_0 is to give a clear description. One can see an increasing trend of N_0 with increasing centrality. The fact is that in more central collisions more particles are involved in interaction which results in larger multiplicity after the collision reaction, where in peripheral collisions the participants in the interaction reduce and hence it results in lower rate of multiplicity. N_0 is also observed to be dependent on the mass of the particle. Massive particles correspond to lower N_0 which means that the multiplicity for massive particles
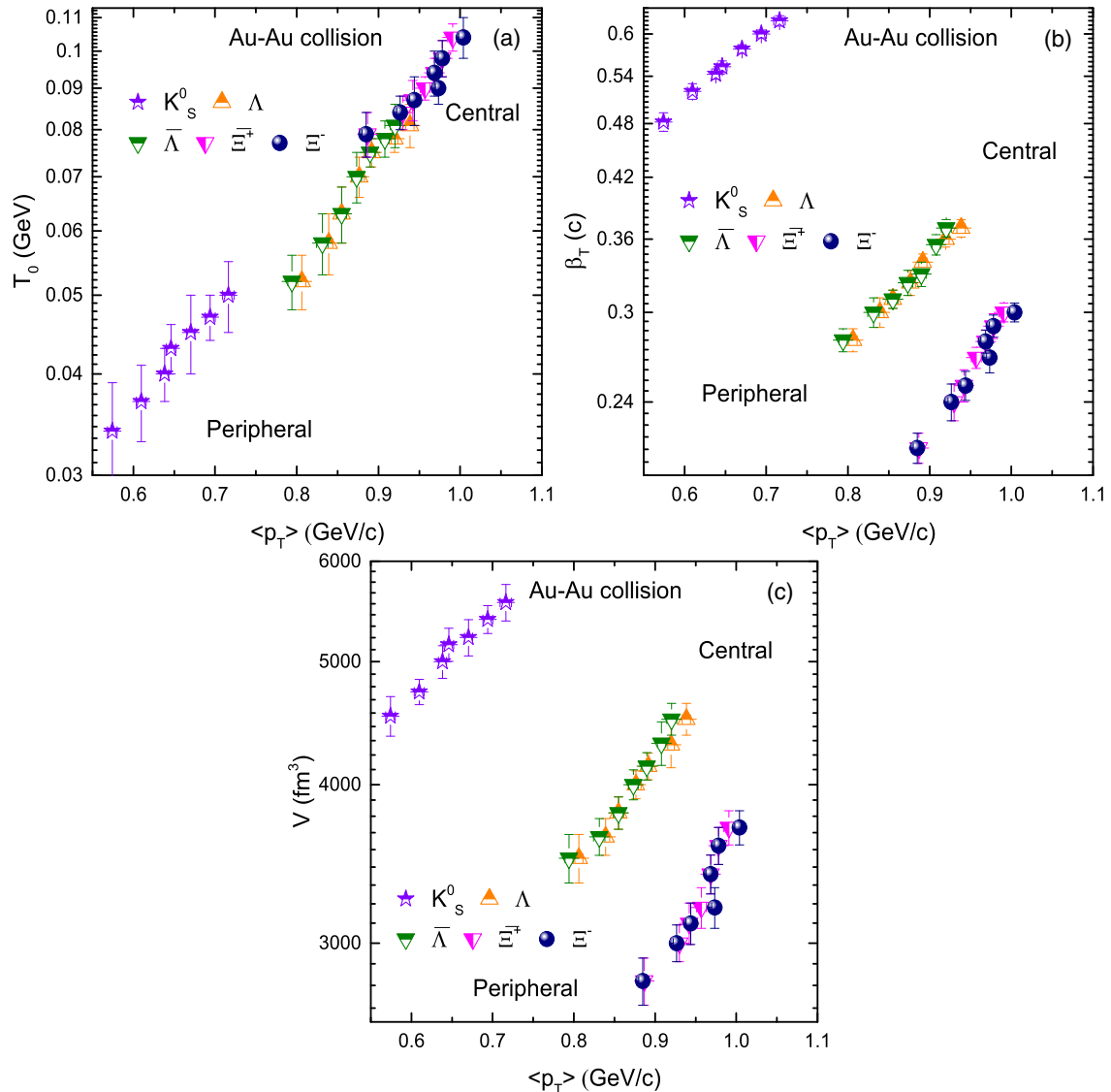

FIG. 6. Correlation of (a) T_0 versus $\langle p_T \rangle$, (b) β_T versus $\langle p_T \rangle$, and (c) V versus $\langle p_T \rangle$.

is less. For instance in the present work, $\bar{\Xi}^+$ and Ξ^- has lower multiplicity and K_s^0 has larger multiplicity, while Λ, $\bar{\Lambda}$ lies in between.

Figure 4 is the same as Figs. 2 and 3, but it demonstrates the dependence of mean p_T ($\langle p_T \rangle$) on centrality and m_0. We see that $\langle p_T \rangle$ increases from K_S^0 to Λ and then Ξ, which manifests that the radial flow effect increases with particle mass. Besides, $\langle p_T \rangle$ is observed to decrease with the decrease of event centrality which renders that the amount of energy gained by nucleons in the system in central collision is large that leads to further multiple scatterings. Whereas, the system in peripheral collisions has an opposite result. The larger $\langle p_T \rangle$ in central collision is an indication of immense radial flow effects in more central collisions. Figure 5 shows the correlation of T_0 and β_T, T_0 and V, and β_T and V.

Figure 5(a) presents the correlation of T_0 and β_T for all under studied particles. The symbols represent different particles and the trend of symbols from up to downward show the trend of correlation from central to peripheral collisions. One can see that there is a positive correlation between T_0 and β_T. T_0 increases with the increase of β_T. In central collision larger T_0 and β_T, which means that central collision systems gains higher degree of excitation which results in larger T_0 and a rapid expansion (harsh squeeze) which corresponds to larger β_T. This result validates our previous results [78]. Panel (b) shows the correlation of T_0 and V. It is observed that like T_0 and β_T, T_0, and V also have a positive correlation. It can be explained as the higher degree of excitation results in larger T_0 due to violent collision as large number of participants are involved in interaction, which results in large multiplicity and hence
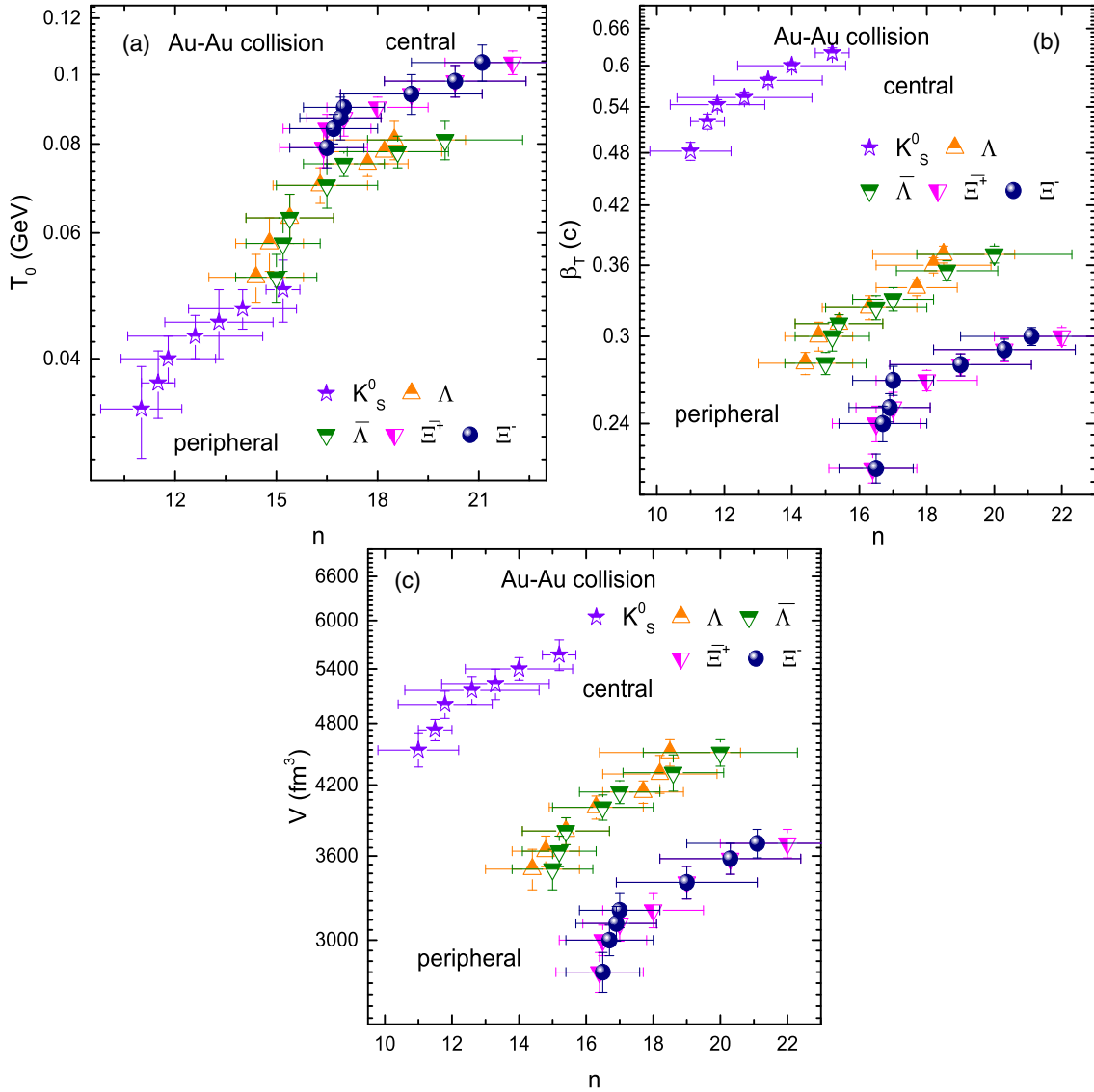

FIG. 7.   Correlation of (a) T_0 versus n, (b) β_T versus n, and (c) V versus n.

lager V. While panel (c) shows the correlation of β_T and V and they also have a positive correlation. Because of very violent collisions, more energy is deposited in the system, which naturally results in larger multiplicity, and correspondingly the fireball expands rapidly (larger β_T).

Figure 6 is similar to Fig. 5, but it displays the correlation among T_0 and $\langle p_T \rangle$, β_T and $\langle p_T \rangle$, and V and $\langle p_T \rangle$. Figure 6(a) shows the correlation of T_0 and $\langle p_T \rangle$. One can see that the correlation between T_0 and $\langle p_T \rangle$ is positive. Similarly in panels (b) and (c), the correlation between β_T and $\langle p_T \rangle$, and V and $\langle p_T \rangle$ is also positive. The positive correlation of β_T and $\langle p_T \rangle$ suggests that more energy is stored per nucleon in the system due to transfer of large amount of energy during collision which results in a rapid expansion of the system (large β_T). The parameters T_0 and V are directly related to the freeze-out of the particles. Therefore the positive correlation of T_0 and $\langle p_T \rangle$ renders that the larger $\langle p_T \rangle$ (energy) transfer to the system occurs due to the violent collision that corresponds to a higher degree of excitation and results in larger T_0. We observed that Λ and $\bar{\Lambda}$ in the most central collisions coincides with $\bar{\Xi}^+$ and Ξ^- in the most peripheral collisions which may suggest the similar thermodynamic nature of Λ and $\bar{\Lambda}$ in the central collisions with $\bar{\Xi}^+$ and Ξ^- in peripheral collisions. On the other hand the positive correlation of V and $\langle p_T \rangle$ renders that larger energy transfer in the system results in large multiplicity which naturally results in larger V if the density saturates. Or the second explanation maybe the larger transfer of energy results in longer evolution time and then larger partonic system, and hence larger V. The correlations in Fig. 6 validate our above results.

Figure 7 is similar to Fig. 6, but it presents the correlation of T_0, β_T, and V with n. Panel (a) shows the correlation of T_0 and n, panel (b) shows the correlation of β_T and n, while panel (c) shows the correlation of V and n. In all panels, a positive correlation among the relevant parameters can be seen.

The positive correlation of entropy based parameter n with T_0 and V renders that larger T_0 in central collisions can be explained as the short lived fireball in central collisions which results in the early freeze-out of the particles in central collisions, and the freeze-out happens when the system is in equilibrium which means larger n. In addition, central collisions are responsible for more number of particles to be involved in interaction where there are large number of binary scattering which results in large V and systems with binary scatterings comes to equilibrium quickly and hence larger n. We have seen that heavier particles have larger T_0 and n and smaller V, and hence they freeze-out earlier than the lighter particles. In addition, along with T_0 in central collisions, β_T is also larger and shows a rapid expansion of the fireball which means that the lifetime of the fireball is not long in central collisions compared to the peripheral collisions. Therefore, in the present work, a longer-lived fireball

corresponds to less β_T and T_0 in peripheral collisions where the system is far from equilibrium and the particles freeze-out later.

IV. CONCLUSIONS

We summarize our main conclusions here;
(a) We reported the transverse momentum spectra of K_s^0, Λ, $\bar{\Lambda}$, $\bar{\Xi}^+$, and Ξ^- in different centrality intervals at 54.4 GeV. The modified hagedorn function with embedded flow is used to fit the experimental data of STAR Collaboration and obtained the freeze-out parameters by using the least-squares method.
(b) We obtained the results for kinetic freeze-out temperature (T_0), transverse-flow velocity (β_T), kinetic freeze-out volume (V), entropy parameters (n), the multiplicity parameter (N_0), and mean transverse momentum ($\langle p_T \rangle$). It is observed that all of these parameters are larger in central collisions and decrease towards periphery.
(c) We reported the decreasing trend of T_0 with the decrease of centrality due to the fact that the number of hadrons involved in interaction decrease from central to peripheral collisions, which correspond to a decrease in the degree of excitation of the system towards periphery and resultantly T_0 decreases.
(d) We also reported the decreasing trend of β_T with the decrease of centrality due to the fact that central collision deposits more energy per nucleon in the system that results in rapid expansion of the fireball. The largest β_T in central collisions show that there is a high pressure gradient in central collisions.
(e) A decreasing trend of V with decreasing centrality is observed and the fact behind this is that the number of participants in the interaction decrease towards periphery and therefore the binary collisions by the rescattering of partons decreases from central to peripheral collisions. n is the smallest for K_s^0 which means that it interacts less with the medium produced in the collision.
(f) The entropy based parameter (n) is also studied and its decreasing trend from central to peripheral collisions is seen, which indicates a larger n (smaller entropy) in central collision, which is evidence that central collisions are closer to the equilibrium state, while n decrease towards periphery and the system goes away from the equilibrium state.
(g) The multiplicity parameter (N_0) decreases from central to peripheral collisions because the central collisions are more harsh reactions and naturally they correspond to larger multiplicity, however it decreases towards periphery because the collisions becomes less violent towards periphery.
(h) We also calculated the mean transverse momentum which decreases from central collision to periphery due to the reason that in central collisions more

energy is deposited in the system, while this deposition of energy decreases towards periphery. The decrease of $\langle p_T \rangle$ towards periphery show that the radial flow effect decrease when the system moves toward the peripheral collisions. $\langle p_T \rangle$ is also observed to be larger for the heavier particle which shows the effect of radial flow is larger in heavier particles.

(i) T_0, β_T, V, n, N_0, and $\langle p_T \rangle$ are mass dependent. T_0, n, and $\langle p_T \rangle$ increase while β_T, V, and N_0 decrease with the increasing rest mass of the particle. The increase of T_0 and decrease of V with m_0 indicate the multiple kinetic freeze-out and volume differential kinetic freeze-out scenarios, respectively.

(j) We reported that there is a positive correlation among T_0 and β_T, T_0 and V, and β_T and V. In addition, the correlation of $\langle p_T \rangle$ with T_0, β_T and V is also checked and is seen to be positive. We also noticed the positive correlation of the entropy based

parameter n with T_0, β_T, and V. In the correlation of β_T and V, the most peripheral collisions of Λ, Λ^- are seen to coincide the most central collisions of $\bar{\Xi}^+$ and Ξ^-. This is similar to the case of the correlation among T_0 and $\langle p_T \rangle$. This is maybe the indication of their similar thermodynamic nature.

[1] J. Adams *et al.* (STAR Collaboration), Nucl. Phys. **A757,** 102 (2005).

[2] K. J. Eskola, in *Proceedings of the International Europhysics Conference on High energy physics (EPS-HEP 1999): Tampere, Finland, 1999*, 231C250 (1999), arXiv: hep-ph/9911350.

[3] S. A. Bass, M. Gyulassy, H. Stoecker, and W. Greiner, J. Phys. G **25,** R1 (1999).

[4] J.-P. Blaizot and J.-Y. Ollitrault, Phys. Rev. Lett. **77,** 1703 (1996).

[5] U. W. Heinz, Nucl. Phys. **A721,** C30 (2003).

[6] P. P. Bhaduri, AAPPS Bull. **30,** 14 (2020).

[7] Garima, P. K. Deshwal, and M. K. Yadav, AIP Conf. Proc. **2352,** 030004 (2021).

[8] T. Niida and Y. Miake, AAPPS Bull. **31,** 12 (2021).

[9] B. Alessandro *et al.* (NA50 Collaboration), Eur. Phys. J. C **39,** 335 (2005).

[10] R. Arnaldi *et al.* (NA60 Collaboration), Phys. Rev. Lett. **99,** 132302 (2007).

[11] T. Song, H. Berrehrah, D. Cabrera, J. M. Torres-Rincon, L. Tolos, W. Cassing, and E. Bratkovskaya, Phys. Rev. C **92,** 014910 (2015).

[12] O. Philipsen, Prog. Part. Nucl. Phys. **70,** 55 (2013).

[13] R. Rapp, Proc. Sci., HardProbes2018 (**2019**) 029.

[14] K. Gallmeister, M. Beitel, and C. Greiner, Phys. Rev. C **98,** 024915 (2018).

[15] C. Plumberg and U. Heinz, Phys. Rev. C **98,** 034910 (2018).

[16] H. Petersen, D. Oliinychenko, M. Mayer, J. Staudenmaier, and S. Ryu, Nucl. Phys. **A982,** 399 (2019).

[17] M. Bleicher, B. Bäuchle, S. Endres, T. Lang, and G. Gräf, Acta Phys. Pol. B Proc. Suppl. **7,** 173 (2014).

[18] L. G. Pang, K. Zhou, N. Su, H. Petersen, H. Stöcker, and X. N. Wang, Nucl. Phys. **A982,** 867 (2019).

[19] Z. Tu (CMS Collaboration), Nucl. Phys. **A982,** 527 (2019).

[20] I. Karpenko and F. Becattini, Nucl. Phys. **A982,** 519 (2019).

[21] M. Nahrgang, M. Bluhm, T. Schaefer, and S. A. Bass, Phys. Rev. D **99,** 116015 (2019).

[22] X.-N. Wang, Proc. Sci., High-pT2019 (**2020**) 040 [arXiv: 1906.11998].

[23] B. Schenke, C. Shen, and P. Tribedy, Phys. Rev. C **99,** 044908 (2019).

[24] J. Cleymans, H. Oeschler, K. Redlich, and S. Wheaton, Phys. Rev. C **73,** 034905 (2006).

[25] P. Braun-Munzinger and J. Stachel, Nature (London) **448,** 302 (2007).

[26] J. Adam *et al.* (STAR Collaboration), Phys. Rev. C **101,** 014916 (2020).

[27] J. Adam *et al.* (STAR Collaboration), Phys. Rev. C **102,** 034909 (2020).

[28] M. Waqas, F. H. Liu, R. Q. Wang, and I. Siddique, Eur. Phys. J. A **56,** 188 (2020).

[29] M. U. Ashraf (STAR Collaboration), Nucl. Phys. **A1005,** 121815 (2021).

[30] Q. Wang, F. H. Liu, and K. K. Olimov, Front. Phys. **9,** 792039 (2021).

[31] M. Waqas and F. H. Liu, Eur. Phys. J. Plus **135,** 147 (2020).

[32] J. Cleymans and K. Redlich, Phys. Rev. C **60,** 054908 (1999).

[33] W. Florkowski and W. Broniowski, Phys. Lett. B **477,** 73 (2000).

[34] P. Braun-Munzinger, J. Stachel, and C. Wetterich, Phys. Lett. B **596,** 61 (2004).

[35] P. P. Yang, M. Y. Duan, F. H. Liu, and R. Sahoo, Symmetry **14,** 1530 (2022).

[36] L. L. Li, F. H. Liu, and K. K. Olimov, Entropy **23,** 478 (2021).

[37] L. L. Li, F. H. Liu, M. Waqas, and M. Ajaz, Universe **8,** 31 (2022).

[38] R. F. Si, H. L. Li, and F. H. Liu, Adv. High Energy Phys. **2018**, 7895967 (2018).

[39] M. Waqas, F. H. Liu, S. Fakhraddin, and M. A. Rahim, Indian J. Theor. Phys. **93**, 1329 (2019).

[40] M. Waqas and G. X. Peng, Entropy **23**, 488 (2021).

[41] M. Waqas, H. M. Chen, G. X. Peng, A. A. K. H. Ismail, M. Ajaz, Z. Wazir, R. Shehzadi, S. Jamal, and A. AbdelKader, Entropy **23**, 1363 (2021).

[42] M. Ajaz, M. Waqas, G. X. Peng, Z. Yasin, H. Younis, and A. A. K. Haj Ismail, Eur. Phys. J. Plus **137**, 52 (2022).

[43] K. K. Olimov, F. H. Liu, K. A. Musaev, and M. Z. Shodmonov, Universe **8**, 174 (2022).

[44] Z. Tang, Y. Xu, L. Ruan, G. van Buren, F. Wang, and Z. Xu, Phys. Rev. C **79**, 051901 (2009).

[45] S. Chatterjee, S. Das, L. Kumar, D. Mishra, B. Mohanty, R. Sahoo, and N. Sharma, Adv. High Energy Phys **2015**, 349013 (2015).

[46] S. Chatterjee, B. Mohanty, and R. Singh, Phys. Rev. C **92**, 024917 (2015).

[47] D. Thakur, S. Tripathy, P. Garg, R. Sahoo, and J. Cleymans, Adv. High Energy Phys. **2016**, 4149352 (2016).

[48] S. Chatterjee and B. Mohanty, Phys. Rev. C **90**, 034908 (2014).

[49] M. Waqas and F. H. Liu, Indian J. Theor. Phys. **96**, 1217 (2022).

[50] M. Waqas, G. X. Peng, F. H. Liu, and Z. Wazir, Sci. Rep. **11**, 20252 (2021).

[51] M. Waqas, G. X. Peng, and F. H. Liu, J. Phys. G **48**, 075108 (2021).

[52] G. Che, J. Gu, W. Zhang, and H. Zheng, J. Phys. G **48**, 095103 (2021).

[53] M. Waqas and G. X. Peng, Adv. High Energy Phys. **2021**, 6674470 (2021).

[54] M. Waqas, G. X. Peng, Z. Wazir, and H. Lao, Int. J. Mod. Phys. E **30**, 2150061 (2021).

[55] H. L. Lao, F. H. Liu, B. C. Li, and M. Y. Duan, Nucl. Sci. Tech. **29**, 82 (2018).

[56] R. Hagedorn, Riv. Nuovo Cimento **6N10**, 1 (1983).

[57] J. Cleymans and D. Worku, J. Phys. G **39**, 025006 (2012).

[58] I. Sena and A. Deppman, Eur. Phys. J. A **49**, 17 (2013).

[59] A. Adare *et al.* (PHENIX Collaboration), Phys. Rev. D **83**, 052004 (2011).

[60] P. K. Khandai, P. Sett, P. Shukla, and V. Singh, Int. J. Mod. Phys. A **28**, 1350066 (2013).

[61] C. Y. Wong and G. Wilk, Acta Phys. Pol. B **43**, 2047 (2012).

[62] J. Cleymans, G. I. Lykasov, A. S. Parvan, A. S. Sorin, O. V. Teryaev, and D. Worku, Phys. Lett. B **723**, 351 (2013).

[63] J. Cleymans, J. Phys. Conf. Ser. **779**, 012079 (2017).

[64] H. Zheng and L. Zhu, Adv. High Energy Phys. **2016**, 9632126 (2016).

[65] C. Tsallis, J. Stat. Phys. **52**, 479 (1988).

[66] C. Tsallis, Eur. Phys. J. A **40**, 257 (2009).

[67] P. K. Khandai, P. Sett, P. Shukla, and V. Singh, J. Phys. G **41**, 025105 (2014).

[68] C. Tsallis, R. S. Mendes, and A. R. Plastino, Physica (Amsterdam) **261A**, 534 (1998).

[69] T. S. Biro, G. Purcsel, and K. Urmossy, Eur. Phys. J. A **40**, 325 (2009).

[70] G. Bíró, G. G. Barnaföldi, T. S. Biró, K. Ürmössy, and Á. Takács, Entropy **19**, 88 (2017).

[71] G. Bíró, G. G. Barnaföldi, T. S. Biró, and K. Shen, EPJ Web Conf. **171**, 14008 (2018).

[72] R. X. Cao, S. Zhang, and Y. G. Ma, Phys. Rev. C **106**, 014910 (2022).

[73] K. K. Olimov, A. Iqbal, and S. Masood, Int. J. Mod. Phys. A **35**, 2050167 (2020).

[74] K. K. Olimov, F. H. Liu, K. A. Musaev, K. Olimov, B. J. Tukhtaev, B. S. Yuldashev, N. S. Saidkhanov, K. I. Umarov, and K. G. Gulamov, Int. J. Mod. Phys. A **36**, 2150149 (2021).

[75] K. K. Olimov, S. Z. Kanokova, K. Olimov, K. G. Gulamov, B. S. Yuldashev, S. L. Lutpullaev, and F. Y. Umarov, Mod. Phys. Lett. A **35**, 2050115 (2020).

[76] P. K. Khandai, P. Sett, P. Shukla, and V. Singh, Int. J. Mod. Phys. A **28**, 1350066 (2013).

[77] M. Waqas, F. H. Liu, and Z. Wazir, Adv. High Energy Phys. **2020**, 8198126 (2020).

[78] M. Waqas and B. C. Li, Adv. High Energy Phys. **2020**, 1787183 (2020).